Case Study

Interdigitating Dendritic Cell Sarcoma with Aberrant EGFR Expression

Xianfeng Frank Zhao[1,*] and Shiyong Li[2]

[1]Department of Pathology, University of Arizona College of Medicine Phoenix, Phoenix VA Healthcare System, Phoenix, AZ; [2]Department of Pathology and Laboratory Medicine, Emory University School of Medicine, Atlanta, GA.

Abstract: Diagnosis and treatment of interdigitating dendritic cell sarcoma (IDCS), a rare tumor of histiocytic origin, remain a challenge for both pathologists and hematologists/oncologists. Due to its rarity, there is no well-defined therapeutic regimen for this neoplasm. We report a case of IDCS with aberrant expression of epidermal growth factor receptor (EGFR) which was not detected in the normal follicular dendritic cells and interdigitating dendritic cells with immunohistochemistry. Molecular studies of the tumor showed no mutation in either the *EGFR* gene or *KRAS* gene. Our findings suggest that EGFR could be a novel diagnostic biomarker and therapeutic target for IDCS.

Keywords: Epidermal growth factor receptor (EGFR), interdigitating dendritic cell sarcoma (IDCS), *KRAS*

Introduction

Interdigitating dendritic cell sarcoma (IDCS) is an extremely rare neoplasm of histiocytic origin and is characterized by neoplastic proliferation of spindled to ovoid cells with phenotypic features like those of interdigitating dendritic cells (IDCs) [1]. IDCS has been identified in almost all age groups and organ systems [2]. Molecular studies of several IDCS collided with non-Hodgkin lymphomas have failed to reveal any specific genetic or molecular abnormalities resulting from *de novo* IDCSs [2]. Due to lack of clinical trials and their low occurrence, such neoplasms are currently treated by local excision, chemotherapy and radiation [3], depending on the stage. Chemotherapy regimens consist of reagents used for non-Hodgkin lymphomas, such as adriamycin, bleomycin, vinblastine, and dacarbazine (ABVD) [4] or cyclophosphamide, hydroxydaunorubicin (adriamycin), oncovin (vincristine), and prednisone (CHOP) [5]. The success rate of combination therapies is extremely variable, with patient response rates ranging from days to years. Due to its rarity, research interest in IDCS is relatively low and specific therapeutic targets have not yet been identified.

*Correspondence: X. Frank Zhao, 650 E Indian School Road, Main Bldg., Rm. 2131, Phoenix, AZ 85012. Office: 602-277-5551, x6346; Fax: 602-222-2669; Email: xfzhao@arizona.edu

Clinical History

Here we report a case of a 63-year-old military veteran with history of Type 2 diabetes mellitus presented with a parapharyngeal mass in 2016 and diagnosed follicular dendritic cell sarcoma (FDCS), Ann Arbor Stage II in January 2017 with 15 of the 48 lymph nodes positive for tumor. The patient completed a cycle of chemotherapy and radiation in

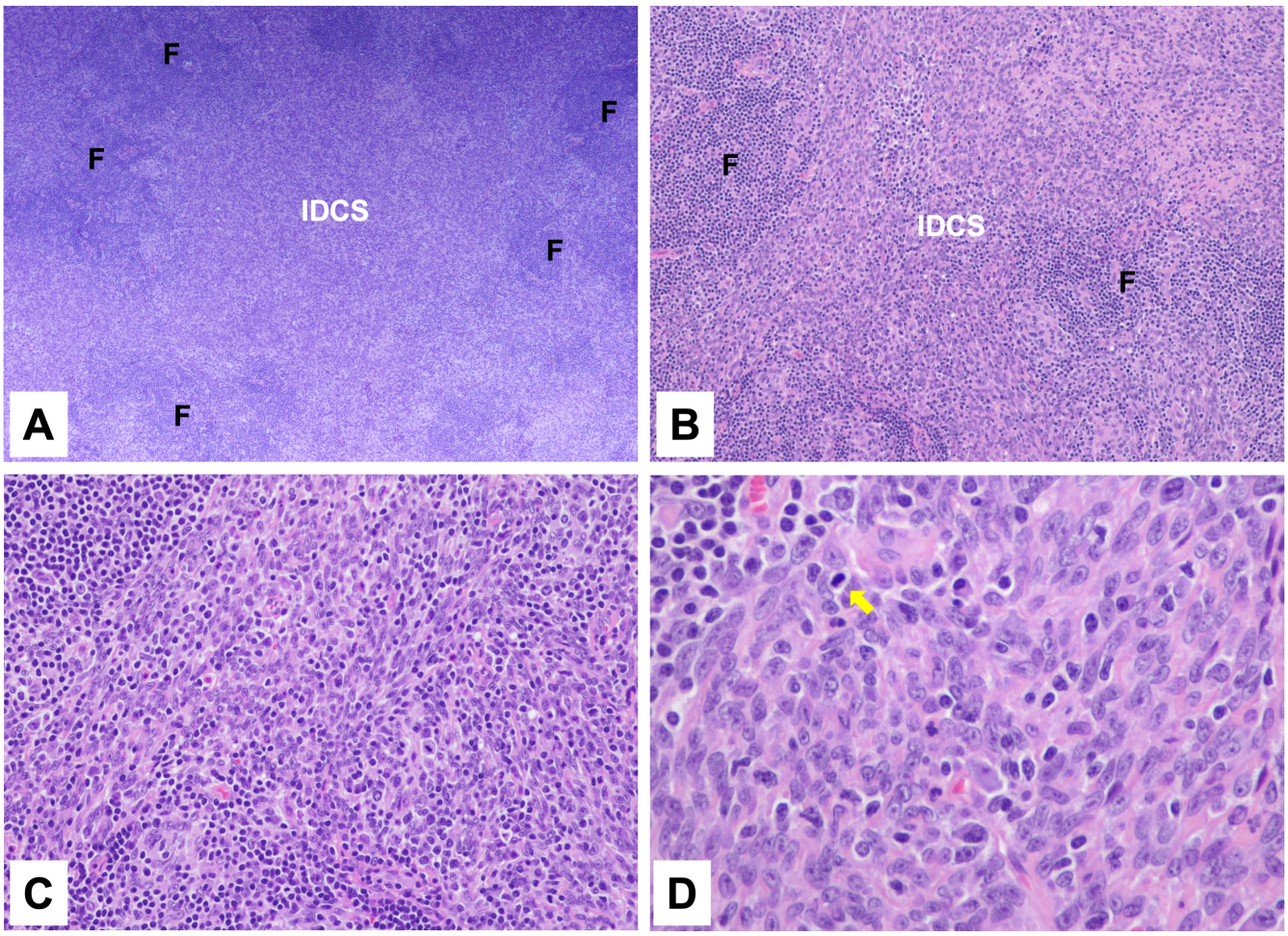

Figure 1: Histology of the IDCS (H&E). A, Nodal architecture completely effaced by a population of oval and spindle cells (magnification x40), pushing the remnant lymphoid follicles to the periphery; B, Parafollicular proliferation of the spindle and oval atypical cells between the remnant lymphoid follicles (**F**) (magnification x100); C, Medium magnification to show the tumor cells with oval or elongated nuclei and small nucleoli (magnification x200); D, High magnification to show the spindle cells with frequent mitotic figures indicated by a yellow arrow (magnification x400).

August 2017 to the right and left side of the neck. PET scan showed negativity in November 2017, but a 7 mm mass showed up at the end of April 2018. The patient was re-biopsied in June 2018 and the workup of the re-biopsied specimen favored the diagnosis of interdigitating dendritic cell sarcoma (ICDS) rather than FDCS. PET-CT scan performed in October 2018 revealed new hypermetabolic lymphadenopathy in the neck, mediastinum, and axillae with interval increase in hypermetabolic activity in the left nasopharynx, extending inferiorly to the oropharynx, suggesting interval progression of metastatic disease. The patient was transferred to an outside cancer center for management and was treated with 6 courses of doxorubicin and dacarbazine for his ICDS. CT scan performed in June 2019 revealed no evidence of disease progression, stable soft tissue density in the right parapharyngeal region, and lung node with

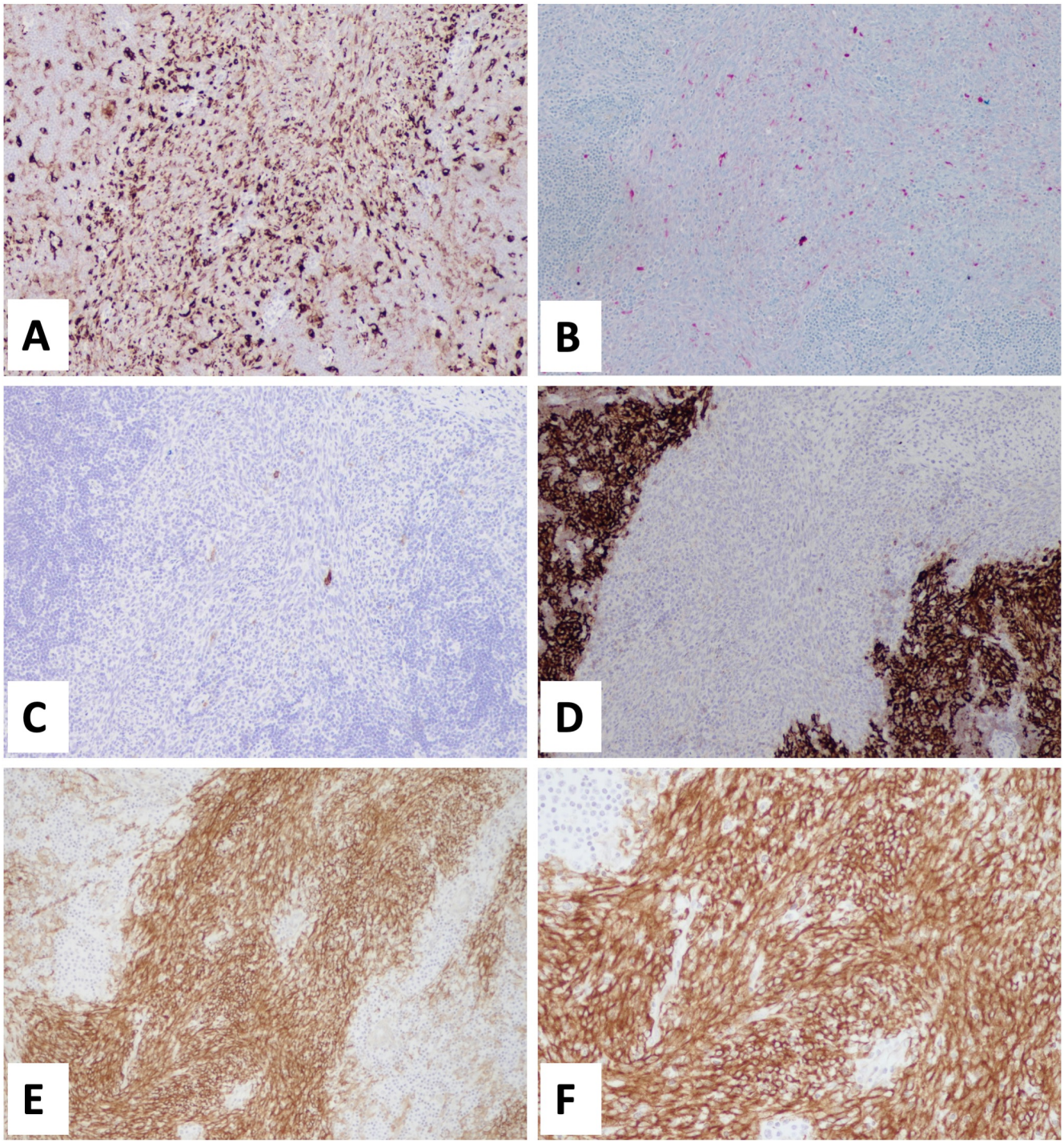

Figure 2: Immunohistochemistry of the IDCS. The IDCS cells are positive for CD68 (A), focally S100 (B), but negative for CD1a (C), and CD21 (D) (magnification x100). Stain for CD21 highlights the follicular dendritic cells in the remnant lymphoid follicles, but the IDCS cells in between are negative (magnification x100). The IDCS cells also show strong membranous staining of EGFR (E, x100; and F, x200).

ground glass appearance, favoring reactive changes. Physical exam showed no oral lesion, or masses in the base of tongue, parotid, and neck. Endoscopically the nasopharynx and larynx look unremarkable. The patient is alive with stable disease.

Materials and Methods

The re-biopsied fresh specimen consisted of a right preauricular lymph node measuring 1.2 x 0.7 x 0.3 cm. Serially sectioning revealed a fish flesh-like surface. Totally submitted for histology, the formalin fixed, and paraffin embedded specimen was sectioned in 2-5 um and stained on a Tissue-Tek Prisma(R) *Plus* Automated Slide Stainer (Sakura Finetek, Torrance, CA) according to the manufacturer's protocol. Immunohistochemistry was performed on a Ventana BenchMark XT automated immunostainer (Ventana, Tucson, AZ) with antibodies from Ventana (CD1a, CD21, CD23, CD35, EMA, HMB45, AE3/5) except for PD1 (Nat105 from Roche Tissue Diagnostics) and EGFR (pharmDxTM from DAKO, Denmark). EBER-ISH was done with an ISH iView Blue Detection Kit. Each IHC or ISH stain was performed with appropriate positive and negative controls.

Small insertion/deletion mutations within exons 19 and 20 of EGFR gene were determined using common fragment analysis [6]. The common driver mutations (see Table 1) of EGFR as well as a few other genes were analyzed using a customized SNaPshot Multiplex System [7]. Briefly, DNA was extracted from the cut tissue rolls, polymerase chain reaction (PCR) was performed using gene-specific primers with different fluorescence tags, and the PCR products were separated using ABI Prism DNA sequencer and analyzed using GeneMapper ID software (Applied Biosystems, Foster City, CA).

Results

The H&E sections showed portions of lymph node completely effaced by a population of ovoid to spindled cells with abundant cytoplasm, ovoid nuclei, and inconspicuous nucleoli. These cells formed fascicles, storiform array, and occasional whorls in the

Table 1: List of genes and common somatic mutations detectable by SNaPshot assay

Genes	Mutations Analyzed
AKT1	c.49G>A (p.Glu17Lys)
BRAF	c.1397G>T (p.Gly466Val), c.1406G>C (p.Gly469Ala), c.1789C>G (p.Leu597Val), c.1799T>A (p.Val600Glu)
EGFR	c.2155G>A (p.Gly719Ser), c.2155G>T (p.Gly719Cys), c.2156G>C (p.Gly719Ala), c.2369C>T (p.Thr790Met), c.2573T>G (p.Leu858Arg), c.2582T>A (p.Leu861Gln)
IDH1	c.394C>A (p.Arg132Ser), c.394C>T (p.Arg132Cys), c.394C>G (p.Arg132Gly), c.395G>A (p.Arg132His), c.395G>T (p.Arg132Leu)
IDH2	c.515G>T (p.Arg172Met)
KRAS	c.34G>A (p.Gly12Ser), c.34G>T (p.Gly12Cys), c.34G>C (p.Gly12Arg), c.35G>A (p.Gly12Asp), c.35G>T (p.Gly12Val), c.35G>C (p.Gly12Ala), c.37G>A (p.Gly13Ser), c.37G>T (p.Gly13Cys), c.37G>C (p.Gly13Arg), c.38G>A (p.Gly13Asp), c.38G>C (p.Gly13Ala), c.181C>A (p.Gln61Lys), c.182A>T (p.Gln61Leu), c.182A>G (p.Gln61Arg), c.183A>T (p.Gln61His), c.183A>C (p.Gln61His)
MEK1	c.167A>C (p.Gln56Pro), c.171G>T (p.Lys57Asn), c.199G>A (p.Asp67Asn)
NRAS	c.181C>A (p.Gln61Lys), c.182A>T (p.Gln61Leu), c.182A>G (p.Gln61Arg)
PIK3CA	c.1624G>A (p.Glu542Lys), c.1633G>A (p.Glu545Lys), c.1633G>C (p.Glu545Gln), c.3140A>G (p.His1047Arg)
PTEN	c.697C>T (p.Arg233*)

parafollicular area (Figure 1A), and they separate the normal lymphocytes and remnant lymphoid follicles into compartments. Mitotic figures were frequently identified (Figure 1D). Immunohistochemical stains showed that the neoplastic cells were CD68+ (Figure 2A), vimentin+, subset lysozyme+, subset MPO+, and subset S100+ (Figure 2B). In addition, the tumor cells also strongly expressed epidermal growth factor receptor (EGFR) in a membranous pattern (Figures 2E & 2F), whereas EGFR was negative in the normal lymph node interdigitating dendritic cells as well as the follicular dendritic cells (both in this tumor and the normal lymph node) (not shown). The tumor cells were negative for CD1a (Figure 2C), CD21 (Figure 2D), CD23, CD35, EBV, EMA, HMB45, AE1/AE3, and PD1. Since the IDCS cells produced EGFR, we also performed molecular studies to determine the insertion/deletion of *EGFR* gene, the somatic mutations of *EGFR* and a few other cancer genes. There were no in-frame deletions in exon 19 or insertions in exon 20 of *EGFR*. SNaPshot multiplex analysis also failed to detect the common driver mutations in *EGFR* or several other targetable genes (Table 1).

Discussion

Aberrant *EGFR* expression has been identified for the first time in the tumor cells of IDCS, and this work may provide a new diagnostic marker as well as a therapeutic target for IDCS. EGFR as a member of receptor tyrosine kinases (TK) recently gained most popularity in non-small cell lung cancers (NSCLC) which are susceptible to various EGFR inhibitors [8]. Our sequencing results showed no mutations in the *EGFR* gene of this IDCS, but the strong aberrant expression of EGFR protein suggests that the humanized monoclonal antibodies are likely effective reagents to treat IDCS. Furthermore, anti-EGFR clinical trials in metastatic colorectal cancers and breast cancers suggest lack of *KRAS* mutation makes such tumors susceptible to these reagents [9]. Even though *EGFR* was shown to be strongly expressed in the IDCS tumor cells, since the humanized monoclonal antibodies have not been approved by FDA to treat IDCS, the oncologist did not treat the patient with any of these humanized antibodies and therefore the therapeutic effect of these reagents is unknown. Clinical trials with more IDCS cases are needed to standardize this potential targeted therapy.

Acknowledgements

The authors claim no conflicts of interest.

Received: September 26, 2020 **Accepted**: September 30, 2020 **Published**: October 26, 2020

References

1. Weiss LM, Chan JKC. Interdigitating dendritic cell sarcoma. In Swerdlow SH, Campo E, Harris NL, Jaffe ES, Pileri SA, Stein H, Thiele J (Eds): WHO Classification of Tumours of Haematopoietic and Lymphoid Tissues (Revised 4th edition). IARC: Lyon 2017. pp. 475-476.
2. Interdigitating dendritic cell sarcoma. PubMed (https://www.ncbi.nlm.nih.gov/pubmed/?term=interdigitating+dendritic+cell+sarcoma). Retrieved on October 30, 2019.
3. Pokuri VK, Merzianu M, Gandhi S, Baqai J, Loree TR, Bhat S. Interdigitating dendritic cell sarcoma. J Natl Compr Canc Netw. 2015; 13: 128-132.
4. Olnes MJ, Nicol T, Duncan M, Bohlman M, Erlich R. Interdigitating dendritic cell sarcoma: a rare malignancy responsive to ABVD chemotherapy. Leuk Lymphoma. 2002; 43: 817-821.
5. Kim SY, Kang JH, Chun SH, et al. Interdigitating dendritic cell sarcoma of the tonsil. Asia Pac J Clin Oncol. 2010; 6: 144-148.
6. Yatabe Y, Hida T, Horio Y, Kosaka T, Takahashi T, Mitsudomi T. A rapid, sensitive assay to detect EGFR mutation in small biopsy specimens from lung cancer. J Mol Diagn. 2006; 8: 335-341.
7. Magnin S, Viel E, Baraquin A, et al. A multiplex SNaPshot assay as a rapid method for detecting KRAS and BRAF mutations in advanced colorectal cancers. J Mol Diagn. 2011; 13: 485-492.
8. da Cunha Santos G, Shepherd FA, Tsao MS. EGFR mutations and lung cancer. Annu Rev Pathol. 2011; 6: 49-69.

9. Seshacharyulu P, Ponnusamy MP, Haridas D, Jain M, Ganti AK, Batra SK. Targeting the EGFR signaling pathway in cancer therapy. Expert Opin Ther Targets. 2012; 16: 15-31.